

Spirals and skyrmions in two dimensional oxide heterostructures

Xiaopeng Li,^{1,2} W. Vincent Liu,^{1,3} and Leon Balents²

¹*Department of Physics and Astronomy, University of Pittsburgh, Pittsburgh, Pennsylvania 15260, USA*

²*Kavli Institute for Theoretical Physics, University of California, Santa Barbara, CA 93106, USA*

³*Center for Cold Atom Physics, Chinese Academy of Sciences, Wuhan 430071, China*

We construct the general free energy governing long-wavelength magnetism in two-dimensional oxide heterostructures, which applies irrespective of the microscopic mechanism for magnetism. This leads, in the relevant regime of weak but non-negligible spin-orbit coupling, to a rich phase diagram containing in-plane ferromagnetic, spiral, cone, and skyrmion lattice phases, as well as a nematic state stabilized by thermal fluctuations.

Introduction. Metallic interfaces between insulating oxides, such as SrTiO₃ (STO)-LaAlO₃ (LAO) or STO-GdTiO₃ (GTO), provide a versatile platform to study two dimensional electron liquids. Numerous experiments have observed magnetism in such structures [1–9], which has generated tremendous interest in emergent many-body phenomena of the interfacial electrons. The mechanism behind the magnetism is presently controversial. Theory has not yet even reached a consensus on whether the magnetic moments arise from localized or extended electrons. Possible explanations include a charge ordered state of interfacial electrons[10, 11], ferromagnetism of a single TiO₂ layer mediated by RKKY coupling from extended subbands[12], fully itinerant magnetism[13], local moment formation assisted by disorder[13], and oxygen defect states[14]. One may even contemplate extrinsic explanations [15].

Despite these uncertainties, the macroscopic properties of the magnetization and its consequences for transport are interesting and require theoretical understanding. In LAO-STO, torque magnetometry measurements indicate in-plane moments with unusual field dependence [2], and significant spin-orbit coupling (SOC) effects are observed [16–18]. Experiments have demonstrated remarkable tunability of electronic properties and phase transitions at the interface [8, 9, 19–21], making this a promising platform to study the interplay of ferromagnetism and SOC. The obvious fact that the presence of an interface breaks inversion symmetry suggests the possibility of analogies to novel helical and skyrmion states studied intensely recently in non-centrosymmetric materials [22] such as MnSi[23], Fe_{0.5}Co_{0.5}Si[24] and magnetic thin films [25–27].

In this article, we take a phenomenological approach based on symmetry, which is valid irrespective of the microscopics. We assume only the SOC is weak (in a precise sense formulated below) and describe the consequences for magnetism. The generic form of the free energy is derived, and includes both anisotropy terms and a linear derivative coupling [28–30] that plays a central role in driving spin modulation instabilities. The general approach is indeed quite analogous to the theory of the skyrmion lattice states just mentioned. Minimizing this

free energy in the weak SOC regime, we find a rich phase diagram (Fig. 1) including in-plane ferromagnetic (FM), spiral, cone, and skyrmion lattice states. The skyrmion lattice state is similar to those discussed above, but has a staggered arrangement of topological skyrmion charge.

To complete our study of the phase diagram, we discuss fluctuation effects based upon renormalization group analysis and general arguments. We determine the universality classes of the various transitions, and more interestingly argue that fluctuations generate a nematic phase between the spiral and paramagnetic ones.

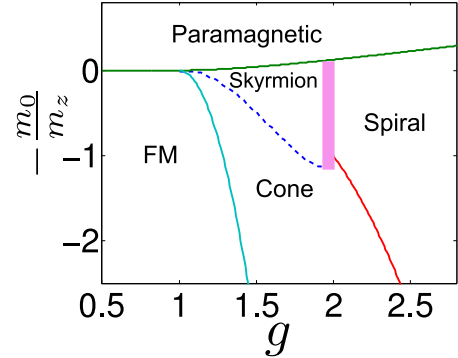


FIG. 1: Mean field phase diagram parametrized by the coupling g and $-\frac{m_0}{m_z}$, which may be taken as a measure of reduced temperature (see text). On lowering the temperature, the paramagnetic phase gives way to in-plane ferromagnetic (FM), spiral, cone, and skyrmion lattice phases, as shown. Solid and dashed lines denote continuous and first order transitions, respectively, as determined by an analysis of critical phenomena. The shaded region marks a narrow sequence of two transitions, as discussed in the text.

Symmetry analysis and free energy. Without SOC, the phenomenological free energy (with Landau coefficients m_0, K and d_0 in standard notation [31]) describing spin fluctuations near a ferromagnetic transition in two dimensions is

$$F_0 = \int d^2\vec{r} \left\{ -m_0 |\vec{S}|^2 + K \sum_{j=x/y} |\partial_j \vec{S}|^2 + d_0 |\vec{S}|^4 \right\}, \quad (1)$$

where $\vec{S}(\vec{r})$ is a three component vector field describing spin density, and we use j to index the two spatial di-

mensions, with sums on repeated indices implied in the following. Here we have neglected the temporal fluctuations, which is valid at non-zero temperature away from quantum critical regime. F_0 has SO(3) spin rotation symmetry. For a square lattice with SOC, *either of atomic or Rashba type*, the symmetry is lower. There is a space-spin combined lattice rotation symmetry C_4 , defined as

$$C_4 : \begin{bmatrix} S_x(\vec{r}) \\ S_y(\vec{r}) \\ S_z(\vec{r}) \end{bmatrix} \rightarrow \mathcal{R}(\alpha) \begin{bmatrix} S_x(R^{-1}(\alpha)\vec{r}) \\ S_y(R^{-1}(\alpha)\vec{r}) \\ S_z(R^{-1}(\alpha)\vec{r}) \end{bmatrix}, \quad (2)$$

with $\mathcal{R} = \begin{bmatrix} R(\alpha) & 0 \\ 0 & 1 \end{bmatrix}$ and $R(\alpha) = \begin{bmatrix} \cos(\alpha) & -\sin(\alpha) \\ \sin(\alpha) & \cos(\alpha) \end{bmatrix}$, where α takes the values of $0, \pi/2, \pi$ or $3\pi/2$. And there is a reflection symmetry \mathcal{R} , where \vec{S} transforms as a pseudovector

$$\mathcal{R} : \begin{bmatrix} S_x(x, y) \\ S_y(x, y) \\ S_z(x, y) \end{bmatrix} \rightarrow \begin{bmatrix} S_x(-x, y) \\ -S_y(-x, y) \\ -S_z(-x, y) \end{bmatrix} \quad (3)$$

Also we have time-reversal symmetry $\mathcal{T} : \vec{S} \rightarrow -\vec{S}$.

The general form of non-SO(3)-invariant terms in the free energy consistent with these symmetries is $F = F_0 + \Delta F$ with

$$\begin{aligned} \Delta F = & \int d^2\vec{r} \{ m_z S_z^2 + \lambda S_z \partial_j S_j \\ & + b_1 [(\partial_x S_y)^2 + (\partial_y S_x)^2] + b_2 \partial_x S_x \partial_y S_y + b_3 \partial_j S_z \partial_j S_z \\ & + d_1 S_z^4 + d_2 S_x^2 S_y^2 + d_3 S_z^2 S_j S_j + \mathcal{O}(\partial^2 S^4, S^6) \}, \quad (4) \end{aligned}$$

where $m_z, \lambda, b_{1,2,3}$ and $d_{1,2,3}$ are phenomenological coupling constants [31]. These terms arise from SOC, and we anticipate $\lambda \propto \mathcal{O}(\lambda_{\text{SO}})$, $m_z \propto \mathcal{O}(\lambda_{\text{SO}}^2)$, and $b_1, b_2, b_3 \propto \mathcal{O}(\lambda_{\text{SO}}^2)$, where λ_{SO} is the microscopic SOC strength. We verify this explicitly for a microscopic model to be discussed elsewhere [32]. However, we note that the theory does not require this scaling, but only that $\lambda, m_z, b_{1,2,3}$ are small for weak SOC. Note that λ is linear in derivatives, which suggests it is possible to lower the energy by forming a state with non-zero wavevector. This is borne out by more detailed analysis, as we will see.

Mean field phase diagram. Near the spin ordering transition temperature T_c the spin configuration is controlled by the quadratic part of the free energy, which reads

$$F^{(2)} = \int \frac{d^2\vec{q}}{(2\pi)^2} T_{\alpha\beta}(\vec{q}) \tilde{S}_\alpha(\vec{q}) \tilde{S}_\beta(-\vec{q}), \quad (5)$$

after a Fourier transformation $S_\alpha(\vec{r}) = \int \frac{d^2\vec{q}}{(2\pi)^2} \tilde{S}_\alpha(\vec{q}) e^{i\vec{q}\cdot\vec{r}}$. The matrix T in Eq. (5) is given by

$$\begin{aligned} T(\vec{q}) = & (-m_0 + K\vec{q}^2) \mathbb{1}_{3 \times 3} \\ & + \begin{bmatrix} b_1 q_y^2 & \frac{b_2}{2} q_x q_y & \frac{i\lambda}{2} q_x \\ \frac{b_2}{2} q_x q_y & b_1 q_x^2 & \frac{i\lambda}{2} q_y \\ -\frac{i\lambda}{2} q_x & -\frac{i\lambda}{2} q_y & m_z + b_3 \vec{q}^2 \end{bmatrix}. \quad (6) \end{aligned}$$

We assume $m_z > 0$, which favors in-plane moments, as typical for 2d systems due to dipolar effects, and in accordance with experiments on LAO-STO [2]. Neglecting for the moment the $b_{1,2,3}$ terms, we obtain the lowest eigenvalue of the T matrix as:

$$\epsilon(\vec{q}) = -m_0 + Kq^2 + \frac{1}{2} \left[m_z - \sqrt{m_z^2 + \lambda^2 q^2} \right] + \mathcal{O}(bq^2). \quad (7)$$

Introducing the dimensionless ratio

$$g \equiv \frac{\lambda^2}{4Km_z},$$

one observes that when $g > 1$, $\epsilon(q)$ is indeed minimized by a non-zero wavevector $q = Q$, where

$$Q = \frac{\lambda}{4K} \frac{\sqrt{g^2 - 1}}{g}.$$

For $g < 1$ the out-of-plane component of the spiral is too costly and the minimum remains at $q = 0$. The corresponding eigenvalue is

$$\epsilon(Q) = -m_0 - \frac{m_z(g-1)^2}{4g} \Theta(g-1), \quad (8)$$

where $\Theta(x)$ is the Heavyside step function.

The couplings $b_{1,2,3}$ can be treated perturbatively, and produce anisotropy in \vec{q} space. The leading order correction to the eigenvalue is

$$\Delta\epsilon(\vec{q}) = \kappa_- b_3 + \kappa_+ (2b_1 + b_2) \frac{q_x^2 q_y^2}{q^4},$$

where $\kappa_\pm = \frac{q^2}{2} (1 \pm m_z / \sqrt{m_z^2 + q^2 \lambda^2}) > 0$. This favors *axial* spirals with wavevectors $\vec{Q}_1 = (Q, 0)$ and $\vec{Q}_2 = (0, Q)$ if $b_1 > -\frac{b_2}{2}$, and *diagonal* spirals with $\vec{Q}_1 = \frac{1}{\sqrt{2}}(Q, Q)$ and $\vec{Q}_2 = \frac{1}{\sqrt{2}}(-Q, Q)$, otherwise.

When $\epsilon(\vec{Q}) < 0$, the system orders, and we introduce two complex order parameters ϕ_1, ϕ_2 by writing

$$\vec{S}(\vec{r}) = \sum_{\nu=1,2} \left[\phi_\nu(\vec{r}) e^{i\vec{Q}_\nu \cdot \vec{r}} \vec{e}_\nu + c.c. \right], \quad (9)$$

where \vec{e}_ν is the eigenvector of T matrix at momentum \vec{Q}_ν . For the axial spiral phases, these are $\vec{e}_1^{\text{axial}} \approx -i \cos(\varphi/2) \hat{x} + \sin(\varphi/2) \hat{z}$, and $\vec{e}_2^{\text{axial}} \approx -i \cos(\varphi/2) \hat{y} + \sin(\varphi/2) \hat{z}$, where $\tan \varphi = \sqrt{g^2 - 1}$. The eigenvectors for diagonal spiral phases are given by a $\pi/4$ rotation as $\vec{e}_\nu^{\text{diag}} = \mathcal{R}(-\frac{\pi}{4}) \vec{e}_\nu^{\text{axial}}$.

The above analysis determines the modes involved in the ordering just below the transition from the paramagnetic state, $\epsilon(Q) = 0^-$ (Eq. (8)), when the magnitude of \vec{S} is infinitesimal. For $g < 1$, this implies in-plane ferromagnetism, while for $g > 1$, there is a degeneracy of states with different choices of ϕ_ν . This is split by quartic terms in the free energy, which can be written as

$$\begin{aligned} f_{\text{spiral}} \approx & 4\epsilon(Q) (\rho_1 + \rho_2) + 4d_0 \left\{ (4 + 2 \cos^2(\varphi)) (\rho_1 + \rho_2)^2 \right. \\ & \left. + 4(1 - 2 \cos(\varphi)) \rho_1 \rho_2 \right\}, \quad (10) \end{aligned}$$

with $\rho_\nu = \frac{1}{2}|\phi_\nu|^2$. Other quartic terms d_1 , d_2 and d_3 are not considered for the reason that they only provide subleading corrections here. From Eq. (10), spin modulations with two components $|\phi_1| = |\phi_2|$ are favorable if $\cos(\varphi) > \frac{1}{2}$; otherwise a spiral phase with $(\phi_1 = 0, \phi_2 \neq 0)$ or $(\phi_1 \neq 0, \phi_2 = 0)$ is favorable. The boundary between these two is at $g = 2$. The spin configuration in the two-component (ϕ_1, ϕ_2) phase is plotted in Fig. 2, showing that it can be regarded as a *skyrmion lattice*, which is a crystalline state of spirals with one spin texture per unit cell. Different from previous skyrmions discussed for other chiral magnets [22, 33, 34], the present skyrmion lattice state has nodal points (Fig. 2), which are protected by the space-spin combined C_4 and time-reversal symmetries. The nodal points can be removed by breaking time-reversal symmetry, for example, with an external magnetic field.

On lowering temperature further, the competition amongst phases shifts, with quartic terms playing a more important role. By a combination of stability analysis of the above ordered states and numerical/analytical minimization of the free energy, we establish the phase diagram in Fig. 1. The minimal free energy states can be approximately expressed in the form

$$\vec{S}(\vec{r}) = \vec{S}_0 + \sum_{\nu=1,2} \left[\phi_\nu(\vec{r}) e^{i\vec{Q}_\nu \cdot \vec{r}} \vec{e}_\nu + c.c. \right],$$

where \vec{S}_0 , ϕ_ν , \vec{e}_ν are parameters that vary in the different phases. Between FM and spiral phases, we obtain a coexistence state, with both \vec{S}_0 and one ϕ_ν non-zero (and $\vec{S}_0 \cdot \vec{e}_\nu = 0$), known as a “cone” state. This state arises due to the competition of linear derivative and quartic terms in the free energy. The boundaries of the cone state with the FM and spiral phases are given respectively by $g = 1 + \sqrt{\frac{2d_2m_0}{d_0m_z}}$ (to leading order in m_0) and $-\frac{m_0}{m_z} = -\frac{1}{2}g(g-1)^2$, and represent continuous transitions. The cone state can also be reached from a skyrmion lattice state by lowering the temperature. The phase transition from the skyrmion lattice to the cone state is found to be first order. An intermediate phase, an anisotropic two-component spiral state, occurs in a narrow transition region between the spiral and skyrmion lattice states (Fig. 1), via a pair of second order transitions.

Fluctuation effects. The above mean-field analysis neglects fluctuation effects, which can be significant in two dimensional systems with continuous broken symmetry. Here we discuss them based upon renormalization group and other arguments.

The in-plane ferromagnetic state, as well as the uniform component of the polarization in the coexistence/cone state, is pinned by anisotropy arising from SOC to lie along one of the easy axes. Thus it behaves as a discrete Ising order parameter and long-range order is thereby stabilized by SOC. The situation is more

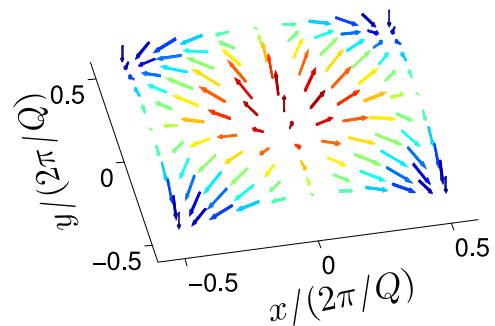


FIG. 2: Spin configuration of an axial skyrmion lattice state. One unit cell is plotted here. Nodal points where the spin moment vanishes, i.e., $S_x = S_y = S_z = 0$, are stable in presence of the space-spin combined C_4 and time-reversal symmetries.

subtle for the spiral states, which have a continuous degeneracy associated with the phase(s) of ϕ_ν . Note that as a result of spatial translation symmetry, the problem has an emergent $U(1) \times U(1)$ symmetry: $\phi_\nu \rightarrow \phi_\nu e^{i\vartheta_\nu}$. This is true for both axial and diagonal spiral phases.

Deep inside the spiral phases, the effect of fluctuations is understood simply by rewriting $\phi_\nu = |\phi_\nu| e^{i\vartheta_\nu}$, and considering quadratic fluctuations of ϑ_ν . These are, as usual, logarithmic, and thereby generate power-law correlations of the non-zero ϕ_ν fields. Thus the spiral order becomes *quasi*-long-range rather than truly static, though the physics is otherwise largely unchanged.

The transitions between the spiral and other phases are more interesting. They can be understood, following the pioneering work of Kosterlitz and Thouless (KT), from the point of view of unbinding of topological defects. This gives rather different results for the two spiral phases.

Consider first the spiral phase, where only a single spiral order parameter is non-zero. The order parameter manifold consists of two disconnected parts, associated to the two possible wavevectors. Here there are two types of topological defects. The first is a vortex in the phase of the spiral, which as usual is a point defect with a logarithmic energy cost (see Fig. S1 in Supplementary Materials). The second is a domain wall separating regions of the two possible spiral wavevectors \vec{Q}_1 and \vec{Q}_2 . This is a defect with a non-zero large tension in two dimensions. The relatively small energy cost of the vortices is readily overcome by entropy, and we expect a conventional KT transition with increasing temperature. For example, the anomalous dimension at this transition is expected to be 1/4.

Since the domain walls are not involved in this transition, their line tension remains positive just above the KT transition, and the system remains in a single “wavevector” domain. Formally, this means the order parameter $\langle \rho_1 - \rho_2 \rangle \neq 0$, so the C_4 rotation symmetry is spontaneously broken, though time-reversal and translation symmetry is restored. Fluctuations therefore induce an

intermediate *nematic* phase between the spiral and paramagnetic phases. The transition from the nematic to paramagnetic state occurs at a higher temperature, and is expected to be of Ising type.

Applying the same reasoning, the transition from the cone to FM phase is also expected to be KT-like. This is consistent because the C_4 symmetry is broken in the FM by the uniform in-plane moment.

Now consider the skyrmion lattice state. Here the order parameter manifold is continuous and fully connected. It is described just by the angular variables ϑ_1 and ϑ_2 , which translate the lattice in either the x or y direction. Consequently, the only defects are vortices in the two phase fields, or equivalently dislocations of the lattice (see Fig. S2 in Supplementary Materials). Therefore only a single transition is expected. This may also be guessed from the fact that the skyrmion lattice preserves C_4 symmetry. The transition should be described as the melting of this skyrmion lattice, which appears to be in the same universality class as the melting of a square lattice on a tetragonal but incommensurate substrate. Such 2d melting transitions were analyzed by Halperin and Nelson, and share similar characteristics with KT transitions [35, 36].

The above conclusions describe likely critical properties based on universality from the general theory of 2d critical phenomena, but for example first order transitions could also occur for non-universal reasons. Hence we vetted them against a non-perturbative but approximate renormalization group (RG) [37] calculation for spiral states, where it is useful to rewrite the free energy (Eqs. (1) and (4)) in terms of slowly-varying order parameters ϕ_ν as

$$F = \int d\vec{r} \left\{ \frac{Z}{2} [(|\partial_x \phi_1|^2 + |\partial_y \phi_2|^2) + \gamma (|\partial_y \phi_1|^2 + |\partial_x \phi_2|^2)] + U(\rho_1, \rho_2) + \mathcal{O}(\partial^4) \right\} \quad (11)$$

To quartic order in the fields, the potential term $U(\rho_1, \rho_2)$ takes the form

$$U(\rho_1, \rho_2) = \frac{u_1}{2} (\rho_1 + \rho_2 - \rho_0)^2 + u_2 \rho_1 \rho_2. \quad (12)$$

The latter can be viewed as simply a rewriting of Eq. (10), and the former following the standard notation [37] allows for slow spatial variations of the spiral order parameters. The theory thus has a momentum cutoff Λ . Symmetries are made transparent in the rewriting form of the free energy. Note that both axial and diagonal spiral phases are described by the same free energy, up to a $\pi/4$ rotation of coordinates.

Introducing dimensionless parameters $\tilde{u}_{1,2} = Z^{-2} \Lambda^{-2} u_{1,2}$, $\tilde{\rho}_0 = Z \rho_0$, from the free energy in Eq. (11), calculations of 1PI RG equations are standard following Ref. [37], and two illuminating limits are given here. First, as $\tilde{\rho}_0$ approaches ∞ , β -functions are asymptotically

$$\beta(\tilde{\rho}_0) = \mathcal{O}(\tilde{\rho}_0^{-2}), \quad \eta = -\Lambda \partial_\Lambda \log Z = \frac{1}{4\pi\sqrt{\gamma}\tilde{\rho}_0} + \mathcal{O}(\tilde{\rho}_0^{-2}),$$

$$\begin{aligned} \beta(\tilde{u}_1) &= (2 - 2\eta)\tilde{u}_1 - \frac{\log 2}{2\pi\sqrt{\gamma}}\tilde{u}_1^2 + \mathcal{O}(\tilde{\rho}_0^{-3}), \\ \beta(\tilde{u}_2) &= (2 - 2\eta)\tilde{u}_2 - \frac{\log 2}{2\pi\sqrt{\gamma}}\tilde{u}_1\tilde{u}_2 + \mathcal{O}(\tilde{\rho}_0^{-3}). \end{aligned} \quad (13)$$

We thus have an approximate fixed line at $\tilde{u}_1^* = \frac{4\pi\sqrt{\gamma}(1-\eta^*)}{\log 2}$, with $\eta^* = \frac{1}{4\pi\sqrt{\gamma}\tilde{\rho}_0}$. This fixed line is parametrized by $\tilde{\rho}_0$. The second limit is $\tilde{\rho}_0 = 0, \gamma \rightarrow 1$, where β -functions are

$$\begin{aligned} \beta(\tilde{u}_1) &= 2\tilde{u}_1 - \frac{\log 2}{\pi\sqrt{\gamma}} \{5\tilde{u}_1^2 + (\tilde{u}_1 + \tilde{u}_2)^2\}, \\ \beta(\tilde{u}_2) &= 2\tilde{u}_2 - \frac{\log 2}{\pi\sqrt{\gamma}} [6\tilde{u}_1 + \tilde{u}_2]\tilde{u}_2 + \mathcal{O}((\gamma - 1)^2). \end{aligned} \quad (14)$$

Here we have $\beta(\tilde{u}_1) = \beta(\tilde{u}_2) = 0$ at the fixed points ($\tilde{u}_1^* = \frac{\pi\sqrt{\gamma}}{3\log 2}, \tilde{u}_2^* = 0$).

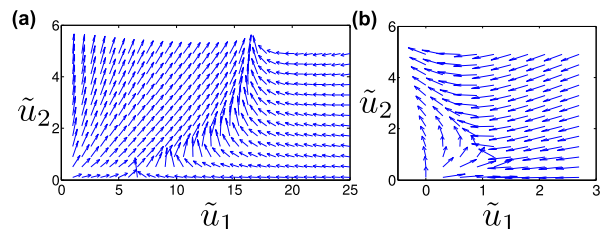


FIG. 3: Vector illustration of $(\beta(\tilde{u}_1), \beta(\tilde{u}_2))$. In this plot we use $\gamma = 1$. In (a) where $\tilde{\rho}_0 = 1$, there is an approximate fixed point at $(\tilde{u}_1^*, \tilde{u}_2^* \rightarrow +\infty)$. In (b), where $\tilde{\rho}_0 = 0$, RG would flow to a regime with $\tilde{u}_1 < 0$. For γ slightly deviated from 1, e.g., $\gamma = 1.5$, the qualitative features of this plot do not change.

In the intermediate regime we solve RG equations numerically and find that $\tilde{\rho}_0$ flows to zero above the KT transition of spiral states when $\tilde{\rho}_0$ is smaller than some critical value $\tilde{\rho}_0^c$, dependent on \tilde{u}_1 and \tilde{u}_2 . Thus we know from the limit (Eq. (14) and Fig. 3 (b)), \tilde{u}_1 flows to negative values and $\tilde{u}_2 > 0$ flows to large positive values above the KT transition, which predicts a nematic phase with an order parameter $\langle \rho_1 - \rho_2 \rangle$. This indicates the nematic phase melts to paramagnetic through a first order phase transition at higher temperature.

Conclusion. We determined a magnetic phase diagram for 2d electron systems with weak but non-negligible SOC, relevant to oxide heterostructures, but which is largely independent of the still unresolved microscopic origin of magnetism. Remarkably, we found a skyrmion lattice phase similar to recent observations in helimagnets. The complex spin textures and nematic state we found should be detectable magnetically (see e.g. the discussion of magnetization of spiral states in Ref.[11]) but also through transport, which should evince spontaneous anisotropy as well as non-linear effects typical in sliding incommensurate spin-density-waves. The influence of Berry phases on electrons [33], e.g. the anomalous Hall effect, is a promising direction for the future. These states may also be relevant to certain schemes for engineering Majorana fermions, which require non-collinear magnetic moments[38].

Acknowledgement. We thank Eun-Gook Moon, Jeremy Levy, Kai Sun for helpful discussions. X.L. would like to thank KITP, UCSB for hospitality and support by NSF PHY11-25915. The work at Pittsburgh is supported by A. W. Mellon Fellowship (X.L.), AFOSR (FA9550-12-1-0079), ARO (W911NF-11-1-0230) and DARPA OLE Program through ARO (X.L. and W.V.L.). L.B. was supported by NSF grant DMR-12-06809.

-
- [1] A. Brinkman, M. Huijben, M. van Zalk, J. Huijben, U. Zeitler, J. C. Maan, W. G. van der Wiel, G. Rijnders, D. H. A. Blank, and H. Hilgenkamp, *Nature Mater* **6**, 493 (2007).
- [2] L. Li, C. Richter, J. Mannhart, and R. C. Ashoori, *Nature Physics* **7**, 762 (2011).
- [3] D. A. Dikin, M. Mehta, C. W. Bark, C. M. Folkman, C. B. Eom, and V. Chandrasekhar, *Phys. Rev. Lett.* **107**, 056802 (2011).
- [4] Ariando, X. Wang, G. Baskaran, Z. Q. Liu, J. Huijben, J. B. Yi, A. Annadi, A. R. Barman, A. Rusydi, S. Dhar, et al., *Nature Communications* **2**, 188 (2011).
- [5] J. A. Bert, B. Kalisky, C. Bell, M. Kim, Y. Hikita, H. Y. Hwang, and K. A. Moler, *Nature Physics* **7**, 767 (2011).
- [6] B. Kalisky, J. A. Bert, B. B. Klopfer, C. Bell, H. K. Sato, M. Hosoda, Y. Hikita, H. Y. Hwang, and K. A. Moler, *Nature Communications* **3**, 922 (2012).
- [7] P. Moetakef, J. R. Williams, D. G. Ouellette, A. P. Kajdos, D. Goldhaber-Gordon, S. J. Allen, and S. Stemmer, *Phys. Rev. X* **2**, 021014 (2012).
- [8] A. Joshua, J. Ruhman, S. Pecker, E. Altman, and S. Ilani, *Proceedings of the National Academy of Sciences* **110**, 9633 (2013).
- [9] F. Bi, M. Huang, C.-W. Bark, S. Ryu, C.-B. Eom, P. Irvin, and J. Levy, *ArXiv e-prints* (2013), 1307.5557.
- [10] R. Pentcheva and W. Pickett, *Physical Review B* **74**, 035112 (2006).
- [11] S. Banerjee, O. Erten, and M. Randeria, *arXiv preprint arXiv:1303.3275* (2013).
- [12] K. Michaeli, A. C. Potter, and P. A. Lee, *Phys. Rev. Lett.* **108**, 117003 (2012).
- [13] G. Chen and L. Balents, *Phys. Rev. Lett.* **110**, 206401 (2013).
- [14] N. Pavlenko, T. Kopp, E. Tsymbal, J. Mannhart, and G. Sawatzky, *Physical Review B* **86**, 064431 (2012).
- [15] D. W. Abraham, M. M. Frank, and S. Guha, *Applied Physics Letters* **87**, 252502 (pages 3) (2005).
- [16] A. D. Caviglia, M. Gabay, S. Gariglio, N. Reyren, C. Cancellieri, and J.-M. Triscone, *Phys. Rev. Lett.* **104**, 126803 (2010).
- [17] M. Ben Shalom, M. Sachs, D. Rakhmilevitch, A. Palevski, and Y. Dagan, *Phys. Rev. Lett.* **104**, 126802 (2010).
- [18] A. Fête, S. Gariglio, A. D. Caviglia, J.-M. Triscone, and M. Gabay, *Phys. Rev. B* **86**, 201105 (2012).
- [19] A. D. Caviglia, S. Gariglio, N. Reyren, D. Jaccard, T. Schneider, M. Gabay, S. Thiel, G. Hammerl, J. Mannhart, and J.-M. Triscone, *Nature* **456**, 624 (2008).
- [20] A. Joshua, S. Pecker, J. Ruhman, E. Altman, and S. Ilani, *Nat Commun* **3**, 1129 (2012).
- [21] C. Cen, S. Thiel, G. Hammerl, C. W. Schneider, K. E. Andersen, C. S. Hellberg, J. Mannhart, and J. Levy, *Nature Materials* **7**, 298 (2008).
- [22] U. K. Roszler, A. N. Bogdanov, and C. Pfleiderer, *Nature* **442**, 797 (2006).
- [23] S. Mühlbauer, B. Binz, F. Jonietz, C. Pfleiderer, A. Rosch, A. Neubauer, R. Georgii, and P. Böni, *Science* **323**, 915 (2009).
- [24] X. Yu, Y. Onose, N. Kanazawa, J. Park, J. Han, Y. Matsui, N. Nagaosa, and Y. Tokura, *Nature* **465**, 901 (2010).
- [25] A. N. Bogdanov and U. K. Rößler, *Phys. Rev. Lett.* **87**, 037203 (2001).
- [26] M. Bode, M. Heide, K. von Bergmann, P. Ferriani, S. Heinze, G. Bihlmayer, A. Kubetzka, O. Pietzsch, S. Blugel, and R. Wiesendanger, *Nature* **447**, 190 (2007).
- [27] S. Heinze, K. von Bergmann, M. Menzel, J. Brede, A. Kubetzka, R. Wiesendanger, G. Bihlmayer, and S. Blugel, *Nat Phys* **7**, 713 (2011).
- [28] I. E. Dzyaloshinskii, *Soviet Physics JETP* **19**, 960 (1964).
- [29] A. N. Bogdanov and D. A. Yablonskii, *Sov. Phys. JETP* **68**, 101 (1989).
- [30] A. Bogdanov and A. Hubert, *Journal of Magnetism and Magnetic Materials* **138**, 255 (1994), ISSN 0304-8853.
- [31] E. M. Lifshitz and L. P. Pitaevskii, *Statistical Physics* (1980).
- [32] X. Li, W. V. Liu, and L. Balents, unpublished.
- [33] S. D. Yi, S. Onoda, N. Nagaosa, and J. H. Han, *Phys. Rev. B* **80**, 054416 (2009).
- [34] J. H. Han, J. Zang, Z. Yang, J.-H. Park, and N. Nagaosa, *Phys. Rev. B* **82**, 094429 (2010).
- [35] D. R. Nelson and B. I. Halperin, *Phys. Rev. B* **19**, 2457 (1979).
- [36] J. M. Kosterlitz and D. J. Thouless, *Journal of Physics C: Solid State Physics* **6**, 1181 (1973).
- [37] J. Berges, N. Tetradis, and C. Wetterich, *Physics Reports* **363**, 223 (2002), ISSN 0370-1573.
- [38] S. Nadj-Perge, I. K. Drozdov, B. A. Bernevig, and A. Yazdani, *Phys. Rev. B* **88**, 020407 (2013).
-

Spirals and skyrmions in two dimensional oxide heterostructures – Supplementary Materials

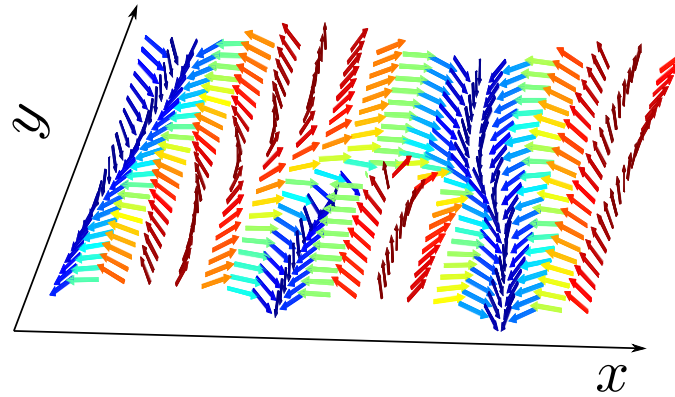


FIG. S1: Spin configuration of a spiral state with one vortex. Spin moments in this spiral state without vortices vary in the x direction and thus form stripes. The presence of a vortex here causes dislocation of the stripe order. Fluctuations of vortices/dislocations tend to restore the translation symmetry.

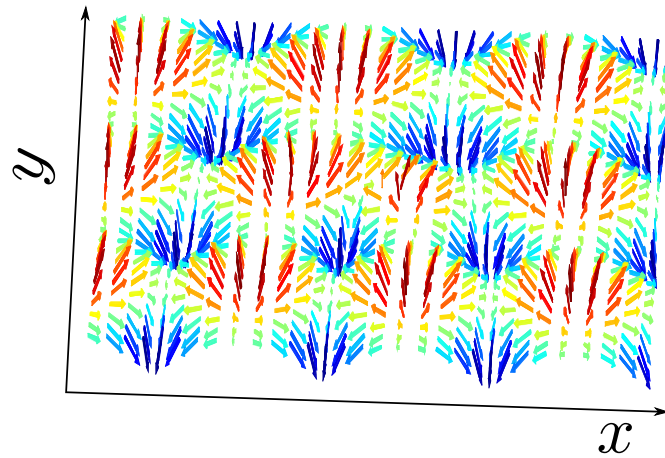


FIG. S2: Spin configuration of a skyrmion lattice state with one vortex. The vortex here causes dislocation of the lattice, fluctuations of which tend to restore the translation symmetry.